Single-Wall Carbon Nanotube Latexes

Markus Antonietti,[†] Yanfei Shen,[†] Takashi Nakanishi,[†,‡] Michael Manuelian,[§] Robert Campbell,[§] Liang Gwee,[||] Yossef A. Elabd,[||] Nikhil Tambe,[⊥] Rene Crombez,[⊥] and John Texter*[,†,⊥]

Max Planck Institute for Colloids and Interfaces, Am Muehlenberg 1, 14476 Golm-Potsdam, Germany, National Institute for Materials Science, 1-2-1 Sengen, Tsukuba 305-0047, Japan, Netzsch Instruments North America, 37 North Avenue, Burlington, Massachusetts 01803, Department of Chemical and Biological Engineering, Drexel University, 3141 Chestnut Street, Philadelphia, Pennsylvania 19104, and Coatings Research Institute, School of Engineering Technology, Eastern Michigan University, Ypsilanti, Michigan 48197

ABSTRACT A nanolatex copolymer (25−30 nm) of an imidalozium bromide acrylate is reported that provides stable waterborne dispersions of single-walled carbon nanotubes (SWCNT) and thermally and electrically conducting coatings that adhere to plastics. This approach to dispersing SWCNT leaps past previous reports by providing stabilization and binder functions simultaneously. Resulting films exhibit 10-fold anisotropy in both thermal and electrical conductivity and appear free of interfacial phonon scattering problems. The electrically conducting networks assembled upon film formation provide a new route to priming plastics for electrodeposition in addition to providing simple antistatic layer formulations. The efficacy of these nanolatexes is assigned to the imidazolium and bromide components shown in other studies to have an affinity for graphene surfaces.

KEYWORDS: carbon nanotubes • charge transport • composites • dielectrics • flexible electronics • latex films

Interest in carbon nanotubes (CNT) has dramatically increased since the first report in 1991 (1) to more than 10^4 publications per year. This interest is focused on realized and anticipated superior electrical, mechanical, optical, thermal, and chemical properties and applications provided by CNT in various environments and hybrid materials. These application areas include nanoelectronics (2, 3), quantum devices (4−6), sensors (7−9), and composite materials of diverse types (10−14).

Although certain nanoelectronic applications such as field-effect transistor sensors may require mechanical manipulation of individual CNT, most medium-tech applications are based on more simple processing steps to create CNT dispersions in water (15−19) or in nonaqueous solvents (20, 21). The dispersion process generally involves two steps, exfoliation of individual or small CNT bundles from larger bundles and the stabilization of these exfoliated entities in a solvent or other phase. Stabilization processes can be characterized as being physical or covalent. Physical methods such as blending or mixing with another phase (22−24) or with a stabilizer (25−27) in another phase are distinguished from surface modifications that covalently modify the CNT to make them stable in a particular solvent or matrix (28, 29). The latter are sometimes accompanied by a deterioration of positive CNT properties.

Waterborne dispersions of CNT remain a focal point for materials development because elimination of organic solvents in coatings and processing operations remains a driver toward more sustainable operations. The most widely used approaches to obtain waterborne CNT dispersions use surfactants (30−36) or polymers (37−48) to stabilize the SWCNT. There have also been several reports on the preparation of latex dispersions of SWCNT (49−51). Grunlan and co-workers reported the use of polyvinylacetate emulsion polymer latexes as binders in coatings of Gum Arabic stabilized SWCNT 29% (w/w) in metal catalyst (49, 50); the effects of the SWCNT and of the metal catalyst on conductivity were not deconvoluted. This approach resulted in a very low percolation threshold to conductivity because of a large excluded volume effect of the emulsion polymer particles. Vandervorst and co-workers prepared SWCNT with COOH surface functionalization and other SWCNT where the COOH groups were esterified with polyvinylalcohol to make them compatible with water (51). These SWCNT were mixed with high T_g and low T_g latexes, and model films were cast and evaluated.

Fukushima and Aida and co-workers (52−54) have shown that imidazolium ionic liquids and polymers are excellent stabilizers for SWCNT in polar and nonpolar media and also promote exfoliation of SWCNT bundles. They demonstrated that SWCNT gels may be obtained by dispersing SWCNT in imidazolium-based ionic liquids. Dropping such gels into water produced stable suspensions without inducing significant precipitation (52, 53). Imidazolium-based ionic liquids were also shown to stabilize SWCNT in vinyl monomer suspensions so that elastic and conducting nanocomposites could be made (54).

* Corresponding author.
Received for review December 30, 2009 and accepted February 09, 2010
[†] Max Planck Institute for Colloids and Interfaces.
[‡] National Institute for Materials Science.
[§] Netzsch Instruments North America.
[||] Drexel University.
[⊥] Eastern Michigan University.
DOI: 10.1021/am900936j

It appears that the imidazolium group, besides having a high tendency to be hydrated and to induce solubilization in water, also has a significant polarizability with respect to the surface of SWCNT. It has also been shown that bromide ion exhibits a binding propensity to graphene sheets (55). One might, therefore, expect that nanolatexes comprising a very high proportion of imidazolium bromide groups may be effective in stabilizing SWCNT.

Here we report the direct preparation of SWCNT nanolatex (25−30 nm) dispersions by mixing and joint ultrasonication, resulting in well dispersed systems with SWCNT concentrations of about 0.5% by weight. This is competitive with the most concentrated aqueous suspensions reported (43, 49, 51, 56) and 5−100 fold more concentrated than most of the surfactant (35, 36) and polymer (38, 40, 41, 44, 45, 48, 57−59) stabilization and dispersion studies in water previously reported. One of these dispersions was concentrated to 1.37% w/w and appears to be the most concentrated aqueous SWCNT dispersion documented to date.

Our nanolatex was prepared by microemulsion polymerizaton (60−62) in the ternary water, IL-Br, and MMA (methylmethacrylate) system at a weight fractional composition of 0.933, 0.040, and 0.027 for water, IL-Br, and MMA, respectively. IL-Br is 1-(2-acryloyloxyundecyl)-3-methylimidazolium bromide:

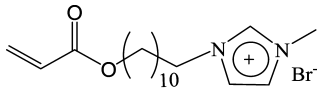

IL-Br

The nanolatex was concentrated to 15−20% by ultrafiltation. A TEM of this nanolatex is illustrated in the Supporting Information.

We prepared a dispersion of cleaned SWCNT in the above latex by adding 3.98 g of nanolatex (14.5% solids) to 21.2 mg of cleaned SWCNT for a crude dispersion 0.527% in SWCNT. The SWCNT remained at the bottom of the mixture. We next subjected the mixture to very mild ultrasonication for 2 min, using a small ultrasonic cleaning bath. The tightly bundled and shiny SWCNT solids expanded to a gray and fuzzy mass, indicating the onset of exfoliation. We then initiated a regimen of more intense ultrasonication using a microtip immersed in the dispersion for various time intervals. After various cumulative dose times a drop of dispersion was taken, diluted, and the optical density was measured. These optical densities are illustrated in Figure 1 as a function of dose time, and show that the degree of dispersion steadily increased throughout the treatment period. The sonication was stopped after 840 s so that two thin wafers of SWCNT nanolatex could be cast for further thermal and electrical conductivity measurements.

Using the extinction coefficient of SWCNT at 500 nm (63) of 28.6 cm^2/mg, we would expect a maximum optical density of 143 if the sample were completely dispersed. The optical density of 79.5 in Figure 1 suggests the illustrated treatment has reached a state of dispersion 56% of the theoretical maximum. The TEM of Figure 2 show that the state of dispersion is extensive but not complete. Figure 2a shows a largely exfoliated bundle with exfoliation in progress at the ends of small bundles. Figure 2b shows an in-plane aggregate of SWCNT formed on drying with individual SWCNT 2 nm in diameter and smaller.

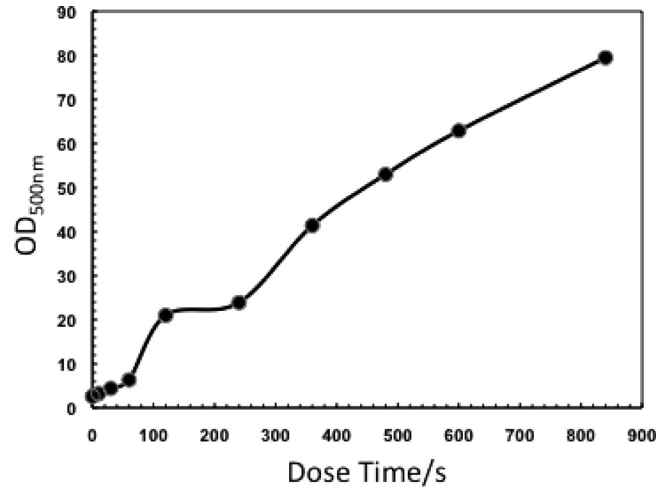

FIGURE 1. Equivalent optical density at 500 nm as a function of ultrasonic dose time for 0.5% w/w dispersion of SWCNT in aqueous nanolatex. Drops of dispersion were diluted by factors of 50−160 with DI water and the $OD_{500\ nm}$ was measured in a 1 cm cuvette. The OD values plotted have been corrected for these dilution factors.

The SWCNT nanolatex suspension was then cast into two polypropylene 2.43 cm inner diameter molds (877 mg in one and 892 mg in the other) and allowed to dry at ambient overnight (see the Supporting Information). Each dried to give a shiny black upper surface (the high gloss may be due to sedimentation during drying) and dull black lower surface. A 0% SWCNT latex control was prepared similarly. These latex films were then separated from the polypropylene molds by the mechanical stresses induced by cutting around the outer periphery of the annular cup. These films, approximately 150−200 μm thick, were used for thermal and electrical conductivity measurements.

Thermal diffusivity at 25 °C was determined by using a xenon flash instrument. The results are listed in Table 1 for both through-plane (⊥) and in-plane (||) geometries. The nanolatex control film has an isotropic thermal diffusivity $\alpha = 0.085$ mm^2/s. The corresponding thermal conductivity $k = \alpha\rho C_p = 0.144$ W/m/K ($\rho = 1.19$ g/cm^3; $C_p = 1.425$ J/g/K) is typical of many polymers and latex films (50, 64, 65) .

These films, made by casting, have a SWCNT content of 3.5% w/w after drying. The through-plane thermal diffusivity and thermal conductivity are each increased about 50% relative to the control film without SWCNT. This magnitude of increase appears novel when compared to SWCNT latex composites, where only a 7−10% increase was reported with 3% SWCNT (50) and the cause for the small effect was attributed to large thermal interface resistance also referred to as interfacial phonon scattering. In that system the SWCNT are stabilized in water by Gum Arabic and then mixed with a polydisperse polyvinylacetate latex (50). Similar nanocomposites of MWCNT in waterborne polyurethane

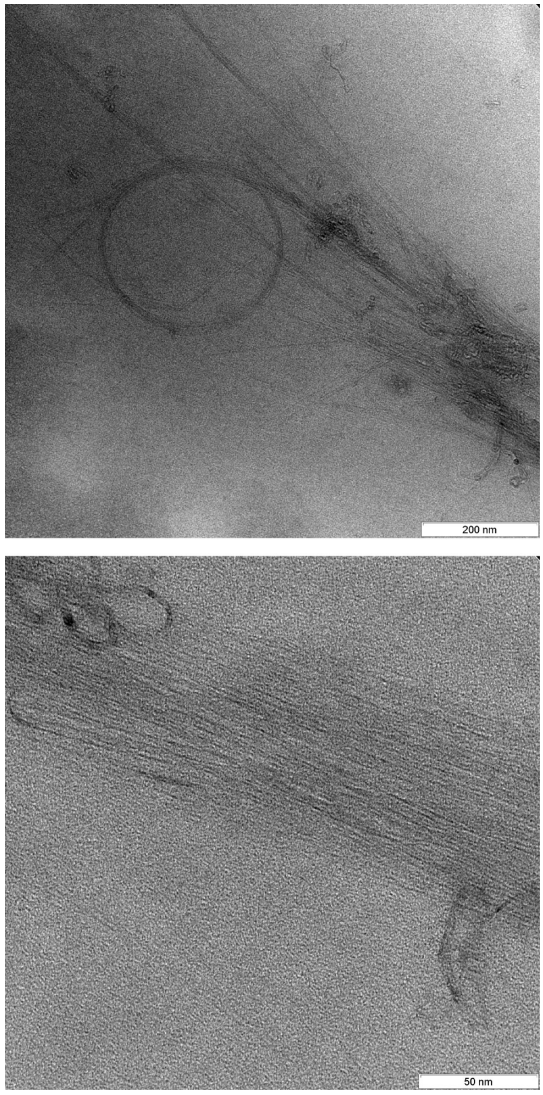

FIGURE 2. Transmission electron micrographs of SWCNTs dispersed in nanolatex after 840 s of cumulative dose. (a) Bundle of SWCNT undergoing exfoliation along with a coiled cluster of SWCNT undergoing exfoliation at the protruding ends; (b) high magnification of exfoliated SWCNT forming a film on drying.

Table 1. Thermal Diffusivity (α) and Thermal Conductivity (*k*) for SWCNT Film (25 °C)

	α (mm^2/s)	*k* (W/m/K)	anisotropy (∥/⊥)
through-plane (⊥)	0.124 ± 0.001	0.322 ± 0.002	8.8
in-plane (∥)	1.086 ± 0.002	2.82 ± 0.003	

(64, 65) exhibit more substantial increases as observed with our nanolatex. Our use of a binder that also is a stabilizer is key to the substantive reduction of interfacial phonon scattering and results from the physical association of the imidazolium bromide groups with the nanographene surface of the SWCNT.

An in-plane thermal diffusivity of 1.086 mm^2/s (Table 1) shows that our use of a nanolatex allows the SWCNT to template the anisotropy. Figure 2b shows that drying after exfoliation can lead to highly anisotropic orientation when highly diluted. The 8.8 fold anisotropy in thermal diffusivity and thermal conductivity was produced by drying and not by any rheological orienting force, although such forces are

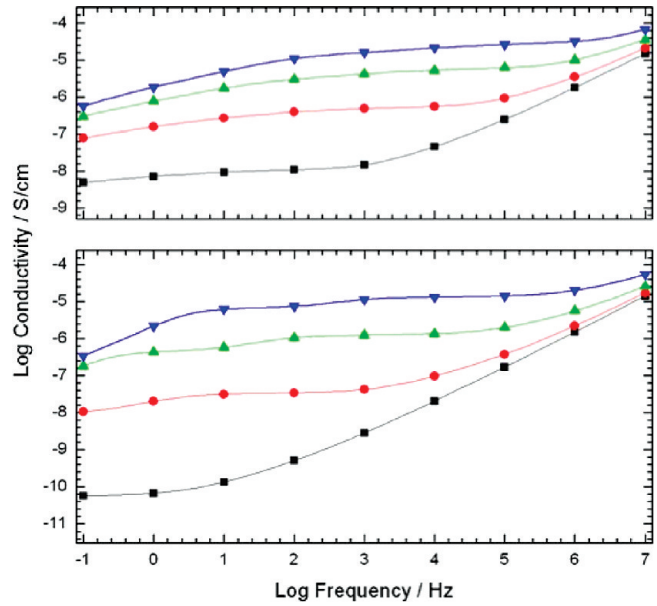

FIGURE 3. Conductivity spectra of cured latex films pre-equiibrated at 44% rh: (top) SWCNT latex film; (bottom) clear latex control film. Spectra measured over 0.1 Hz to 10 MHz. Temperatures vary from −50 to 100 °C: −50 °C (■); −25 °C (•); 0 °C (▲); 25 °C (▼).

commonly encountered in many coating and spinning processes. The films produced by Grunlan and co-workers (49, 50) rely on producing a microheterogeneous material that maintains a basically cubic (isotropic) structure, wherein the SWCNT are directed to interstices between large latex particles. Nanolatexes of what is essentially a hydrogel copolymer produce a more homogeneous film that is templated by the high aspect ratio SWCNT. The room-temperature anisotropy of 8.8 can be compared with that for pyrolytic graphite of 47 (66). The in-plane thermal conductivity of 1.83 W/m/K is a very respectable value in view of the intrinsic value of 210 W/m/K obtained (67) for oriented SWCNT. The 3.5% w/w corresponds to a volume fraction of only 2.5%. The theoretical in-plane conductivity for fully aligned and dispersed SWCNT is (0.975 · 0.144 + 0.025 · 210 =) 5.39 W/m/K. This film, therefore, exhibits an in-plane thermal conductivity about 34% of the maximum achievable at a volume fraction of 0.025.

Through-plane electrical conductivity spectra (see the Supporting Information) obtained for one of these 3.5% w/w SWCNT nanolatex films and for a nanolatex-only sample are illustrated in Figure 3 at various temperatures. This particular type of nanolatex has a significant amount of ionic conductivity due to the high fraction of imidazolium bromide functional groups. However, at each temperature the SWCNT nanolatex conductivity curve lies above the control curve, but the increment decreases from 2 orders of magnitude at −50 °C, to 1 order of magnitude at −25 °C, a factor of 3 at 0 °C, and a smaller difference at 25 °C.

Through-plane and in-plane conductivities were also measured for the same film at 25 °C and at 44% rh using a Solaratron-based impedance spectroscopy system (see the Supporting Information). The in-plane measurements utilized a four-probe technique. A through-plane conductivity of 0.011 mS/cm was obtained and in-plane values of 0.135

Table 2. Electrical Conductivity (σ) for SWCNT Film (25°C; 44% rh)

	σ (mS/cm)	anisotropy (∥/⊥)
through-plane (⊥)	0.009−0.011	
in-plane (∥)		10−15
top	0.135 ± 0.001	
bottom	0.110 ± 0.003	

Table 3. Topcoat Cross-Cut Adhesion Results for Nanolatex-Based Pigmented Primer on ABS (acrylonitrile butadiene styrene resin) Plastic Substrates

topcoat	bare	nanolatex primer
flat latex	35−65% of area detached	small flakes detached along edges and intersections; 5−15% of lattice affected
acrylic-epoxy	>65% of area detached	no detachment

mS/cm and 0.110 mS/cm were obtained for the shiny and dull surfaces, respectively, of the film. The shiny black side was the upper surface that dried in contact with air, and the dull black side is the side that contacted the polypropylene mold during drying.

These results are summarized in Table 2, where we see that an electrical conductivity anisotropy of 10−15 was observed. This anisotropy, as in the earlier examined case of thermal conductivity, results from the nanoscale diameter of the latex particles and the very high anisotropy of the SWCNT. The large size of the latex particle studied by Grunlan and co-workers (49, 50) produced nanocomposites that had higher conductivity, but those systems are restricted to being electrically isotropic. Indeed, when very small latexes were used, a significantly lower conductivity was observed (49). Comparison with SWCNT-doped HDPE indicates the electrical percolation threshold of SWCNT in polymer matrices is at about 3.5% w/w (68). An earlier preparation using lower intensity sonication produced evidence of through-plane network formation with electronic conductivities of about 0.002 mS/cm over −50 to 0 °C. Refinements of the compositions and processes described herein should lead, therefore, to substantial increases in electrical conductivity.

The number of useful applications of such SWCNT nanolatexes is increased because of the excellent adhesion to a variety of substrates provided by the nanolatex. A simple primer was formulated using the nanolatex (see the Supporting Information) to prime acetonitrile-butadiene-styrene resin substrates, overcoating with a topcoat (a flat waterborne latex topcoat and a two-part waterborne acrylic epoxy topcoat), and then applying a cross-cut adhesion tape test. Results are illustrated in Table 3. In both cases, the additional adhesion provided by this nanolatex primer was significant.

A schematic illustrating a possible mechanism of nanolatex stabilization is illustrated by the cartoon in Figure 4. This cartoon illustrates that as exfoliation progresses, the number of surface bonds to exfoliated tubes with imidazolium bromide end groups can increase. The model also

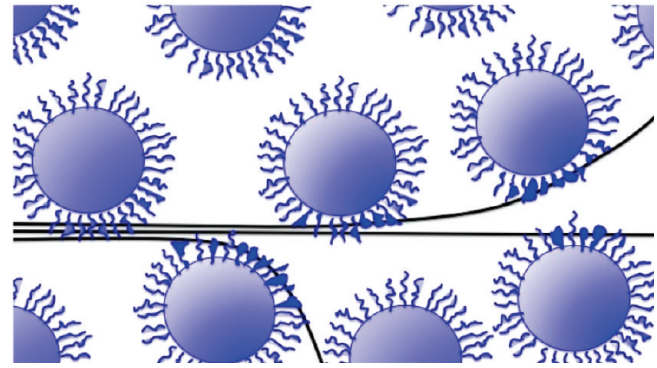

FIGURE 4. Two-dimensional model illustrating possible mechanism of nanolatex stabilization of SWCNT during bundle exfoliation. The nanolatex diameter to SWCNT diameter is approximated at about 27:1 nm in conformity with actual sizes. The mechanism of imidazolium bromide binding is illustrated as occurring through the outermost groups of the nanolatex that bind to the SWCNT partially before exfoliation and more so as the exfoliation progresses.

illustrates how nanolatexes bound to partially exfoliated tubes increase the effective inertia of the exfoliated segments. A 25 nm diameter latex particle has a mass over 2 × 10^6 times greater than a 25 nm length of SWCNT (assuming the latex particle and the SWCNT have equal densities and a 1.2 nm SWCNT diameter). Such an inertial imbalance is expected to promote further exfoliation.

This study has demonstrated that SWCNT are easily dispersed as waterborne latex dispersions at 0.5% by weight. Coatings and castings of such dispersions may be dried to form films approximately 3−3.5% by weight SWCNT. Earlier SWCNT latex dispersion reports cited various means to form stable SWCNT dispersions before mixing in one kind of latex (emulsion polymer) or another (49−51). Our direct approach uses the nanolatex as both a stabilizer and as a binder.

Applications for such conductive films include photothermal coatings for light activated sealing, antistatic discharge layers, ink jet writable conductive layers, and RFID devices, and a general solution to making plastic components more amenable to electrospray and electrodeposition, because only charge generation and not high currents are required.

Acknowledgment. The authors thank Rona Pitschke for providing the TEM images used in this paper. J.T. is indebted to Professor Markus Antonietti for hospitality and support and to the Max Planck Society for their support during his sabbatical leave at the Max Planck Institute of Colloids and Interfaces; J.T. also gratefully acknowledges the support of Eastern Michigan University, Air Force Research Laboratory (UTC Prime Contract FA8650-05-D-5807, Task Order BH Subcontract Agreement 06-S568-BH-C1), and AFOSR Grant FA9550-08-1-0431 for support during his sabbatical leave.

Supporting Information Available: Details of SWCNT cleaning, surfactant synthesis, and nanolatex synthesis, along with sonication details for three different methods used in this study and photos of our initial dispersion and thin film castings; experimental methods for UV/vis, thermal diffusivity, dielectric spectroscopy, impedance spectroscopy, SEM, TEM, and DSC; auxiliary data include conductivity,

permittivity, and dielectric loss spectra of initial SWCNT castings, along with TGA, DSC, and SEM of SWCNT latex films; details and support for the nanolatex adhesion test results. This material is available free of charge via the Internet at http://pubs.acs.org.

REFERENCES AND NOTES

(1) Iijima, S. *Nature* **1991**, *334*, 56–58.
(2) Lu, W.; Lieber, C. M. *Nat. Mater.* **2007**, *6*, 841–850.
(3) Cao, Q.; Rogers, J. A. *Adv. Mater.* **2009**, *21*, 29–53.
(4) Postma, H. W. Ch.; Teepen, T.; Yao, Z.; Grifoni, M.; Dekker, C. *Science* **2001**, *293*, 76–79.
(5) Yang, L.; Chen, J.; Yang, H.; Dong, J. *Phys. Rev. B* **2004**, *69*, 153407.
(6) Akinwande, D.; Nishi, Y.; Wong, H.-S. P. *IEEE Trans. Nanotechnol.* **2009**, *8*, 31–36.
(7) Cosnier, S.; Ionescu, R. E.; Holzinger, M. *J. Mater. Chem.* **2008**, *18*, 5129–5133.
(8) Wang, Y.; Wang, X.; Wu, B.; Zhao, Z.; Yin, F.; Li, S.; Qin, X.; Chen, Q. *Sens. Actuators, B* **2008**, *130*, 809–815.
(9) Heller, D. A.; Jin, H.; Martinez, B. M.; Patel, D.; Miller, B. M.; Yeung, T.-K.; Jena, P. V.; Hoebartner, C.; Ha, T.; Silverman, S. K.; Strano, M. S. *Nat. Nanotechnol.* **2008**, *4*, 114.
(10) Moniruzzaman, M.; Winey, K. I. *Macromolecules* **2006**, *39*, 5194–5205.
(11) Oya, T.; Ogino, T. *Carbon* **2008**, *46*, 169–171.
(12) Miglietta, M. L. in Aciemo, D.; D'Amore, A.; Grassia, L. *IVth International Conference on Times of Polymers (TOP) and Composites*, Ischia, Italy, Sept 21—24, 2008; American Institute of Physics: Lancaster, PA, 2008; pp 210—212.
(13) Peng, C.; Zhang, S.; Jewell, D.; Chen, G. Z. *Prog. Nat. Sci.* **2008**, *18*, 777–788.
(14) Fujigaya, T.; Morimoto, T.; Niidome, Y.; Nakashima, N. *Adv. Mater.* **2008**, *20*, 3610–3614.
(15) Kim, T.-H.; Doe, C.; Kline, S. R.; Choi, S.-M. *Adv. Mater.* **2007**, *19*, 929–933.
(16) Wang, R. K.; Park, H.-O; Chen, W.-C.; Silvera-Batista, C.; Reeves, R. D.; Butler, J. E.; Ziegler, K. J. *J. Am. Chem. Soc* **2008**, *130*, 14721–14728.
(17) Ciofanni, G.; Obata, Y.; Sato, I.; Okamura, Y.; Raffa, V.; Mensiassi, A.; Dario, P.; Takeda, N.; Takeoka, S. *J. Nanopart. Res.* **2009**, *11*, 477–484.
(18) Wang, Z.; Shirley, M. D.; Meikle, A. T.; Whitby, R. L. D; Mikhalovsky, S. V. *Carbon* **2009**, *47*, 73–79.
(19) Moon, Y. K.; Lee, J.; Lee, J. K.; Kim, Ta. K.; Kim, S. H. *Langmuir* **2009**, *25*, 1739–1743.
(20) Smiechowski, M. F.; Lvovich, V. F. *J. Electroanal. Chem.* **2005**, *577*, 67–78.
(21) Shen, J.; Hu, Y.; Qin, C.; Li, C.; Ye, M. *Composites, Part A* **2008**, *39*, 1679–1683.
(22) Xie, X.-L.; Mai, Y.-W.; Zhou, X.-P. *Mater. Sci. Eng. R* **2005**, *49*, 89–112.
(23) Wu, P.; Chen, X.; Hu, N.; Tam, U. C.; Blixt, O.; Zettl, A.; Bertozzi, C. R. *Angew. Chem., Int. Ed.* **2008**, *47*, 5022–5025.
(24) Shih, Y. F.; Chen, L. S. R.; Jeng, J. *Polymer* **2008**, *49*, 4602–4611.
(25) Kong, H.; Luo, P.; Gao, C.; Yan, D. *Polymer* **2005**, *46*, 2472–2485.
(26) Homenick, C. M.; Lawson, G.; Adronov, A. *Polym. Rev.* **2007**, *47*, 265–290.
(27) Hubble, L. J.; Clark, T. E.; Makha, M.; Raston, C. L. *J. Mater. Chem.* **2008**, *18*, 5961–5966.
(28) Qin, S.; Qin, D.; Ford, W. T.; Resasco, D. E.; Herrera, J. E. *J. Am. Chem. Soc.* **2004**, *126*, 170–176.
(29) Choi, J.-Y.; Han, S.-W.; Huh, W.-S.; Tan, L.-S.; Baek, J.-B. *Polymer* **2007**, *48*, 4034–4040.
(30) Patel, N.; Egorov, S. A. *J. Am. Chem. Soc.* **2005**, *127*, 14124–14125.
(31) Vaisman, L.; Wagner, H. D.; Marom, G. *Adv. Colloid Interface Sci.* **2006**, *128—130*, 37–46.
(32) Tomonari, Y.; Murakami, H.; Nakashima, N. *Chem. Eur. J.* **2006**, *12*, 4027–4034.
(33) Rastogi, R.; Kaushal, R.; Tripathi, S. K.; Sharma, A. l.; Kaur, I.; Bharadwaj, L. M. *J. Colloid Interface Sci.* **2008**, *328*, 421–428.
(34) Sáfer, G. A. M.; Ribeiro, H. B.; Malard, L. M.; Plentz, F. O.; Fantini, C; Santos, A. P.; de Freitas-Silva, G.; Idemore, Y. M. *Chem. Phys. Lett.* **2008**, *462*, 109–111.
(35) Wang, Q.; Han, Y.; Wang, Y.; Qin, Y.; Guo, Z.-X. *J. Phys. Chem. B* **2008**, *112*, 7227–7233.
(36) Sun, Z.; Nicolosi, V.; Rickard, D.; Bergin, S. D.; Aherne, D.; Coleman, J. N. *J. Phys. Chem. C* **2008**, *112*, 10692–10699.
(37) Dror, Y.; Pyckhout-Hintzen, W.; Cohen, Y. *Macromolecules* **2005**, *38*, 7828–7836.
(38) Nepal, D.; Geckler, K. E. *Small* **2006**, *2*, 406–412.
(39) Liu, Y.; Liang, P.; Zhang, H.-Y.; Guo, D.-S. *Small* **2006**, *2*, 874–878.
(40) Lee, J. U.; Huh, J.; Kim, K. H.; Park, C.; Jo, W. H. *Carbon* **2007**, *45*, 1051–1057.
(41) Wang, D.; Chen, L. *Nano Lett.* **2007**, *7*, 1480–1484.
(42) Doe, C.; Choi, S.-M.; Kline, S. R.; Jang, H.-S.; Kim, T.-H. *Adv. Funct. Mater.* **2008**, *18*, 2685–2691.
(43) Edri, E.; Regev, R. *Anal. Chem.* **2008**, *80*, 4049–4054.
(44) Noguchi, Y.; Fujigaya, T.; Niidome, Y.; Nakashima, N. *Chem. Phys. Lett.* **2008**, *455*, 249–251.
(45) Yan, L. Y.; Poon, Y. F.; Chan-Park, M. B.; Chen, Y.; Zhang, Q. *J. Phys. Chem. C* **2008**, *112*, 7579–7587.
(46) Xin, X.; Xu, G.; Zhao, T.; Zhu, Y.; Shi, X.; Gong, H.; Zhang, Z. *J. Phys. Chem. C* **2008**, *112*, 16377–16384.
(47) Chen, S.; Jiang, Y.; Wang, Z.; Zhang, X.; Dai, L.; Smet, M. *Langmuir* **2008**, *24*, 9233–9236.
(48) Zou, J.; Liu, L.; Chen, H.; Khondaker, S. I.; McCullough, R. D.; Huo, Q.; Zhai, L. *Adv. Mater.* **2008**, *20*, 2055–2060.
(49) Grunlan, J. C.; Mehrabi, A. R.; Bannon, M. V.; Bahr, J. L. *Adv. Mater.* **2004**, *16*, 150–153.
(50) Grunlan, J. C.; Kim, Y.-S.; Ziaee, S.; Wei, X.; Abdel-Magid, B.; Tao, K. *Macromol. Mater. Eng.* **2006**, *291*, 1035–1043.
(51) Vandervorst, P.; Lei, C.-H.; Lin, Y.; DuPont, O.; Dalton, A. B.; Sun, Y.-P.; Keddie, J. L. *Prog. Org. Coat.* **2006**, *57*, 91–97.
(52) Fukushima, T.; Kosaka, A.; Ishimura, Y.; Yamamoto, T.; Takigawa, T.; Ishiit, N.; Aida, T. *Science* **2003**, *300*, 2072–2074.
(53) Fukushima, T.; Aida, T. *Chem. Eur. J.* **2007**, *13*, 5048–5058.
(54) Sekitani, T.; Noguchi, Y.; Hata, K.; Fukushima, T.; Aida, T.; Someya, T. *Science* **2008**, *321*, 1468–1472.
(55) Mehta, A.; Nelson, E. J.; Webb, S. M.; Jolt, J. K. *Adv. Mater.* **2009**, *21*, 102–106.
(56) Wenseleers, W.; Vlasov, I. I.; Goovaerts, E.; Obraztsova, E. D.; Lobach, A. S.; Bouwen, A. *Adv. Funct. Mater.* **2004**, *14*, 1105–1112.
(57) Shvartzman-Cohen, R.; Florent, M.; Goldfarb, D.; Szleifer, I.; Yerushalmi-Rozen, R. *Langmuir* **2008**, *24*, 4625–4632.
(58) Sinani, V. A.; Gheith, M. K.; Yaroslavov, A. A.; Rakhnyanskaya, A.; Sun, K.; Mamedov, A. A.; Wicksted, J. P.; Kotov, N. A. *J. Am. Chem. Soc.* **2005**, *127*, 3463–3472.
(59) Nepal, D.; Geckeler, K. E. *Small* **2007**, *3*, 1259–1265.
(60) Yan, F.; Texter, J. *Chem. Commun.* **2006**, 2696–2698.
(61) Yan, F.; Texter, J. *Angew. Chem., Int. Ed.* **2007**, *46*, 2440–2443.
(62) England, D. M.S. Thesis, Eastern Michigan University, Ypsilanti, MI, 2008.
(63) Bahr, J. L.; Mickelson, E T.; Bronikowski, M. J.; Smalley, R. E.; Tour, F. M. *Chem. Commun.* **2001**, *193*.
(64) Holman, J. P. *Heat Transfer*, 9th ed.; McGraw-Hill: New York, 2002.
(65) Cai, D.-Y.; Song, M. *Macromol. Chem. Phys.* **2007**, *208*, 1183–1189.
(66) Slack, G. A. *Phys. Rev.* **1962**, *127*, 694–701.
(67) Hone, J.; Llaguno, M. C.; Biercuk, M. J.; Johnson, A. T.; Batlogg, B.; Benes, Z.; Fischer, J. E. *Appl. Phys. A: Mater. Sci. Proc.* **2002**, *74*, 339.
(68) Zhang, Q.; Rastogi, S.; Chen, D.; Lippits, D.; Lemstra, P. J. *Carbon* **2006**, *44*, 778–785.

AM900936J